This is the author's version of an article that has been published in this journal. Changes were made to this version by the publisher prior to publication.
The final version of record is available at http://dx.doi.org/10.1109/LMWC.2015.2496794

A Non-Quasi-Static FET Model Extraction Procedure Using the Dynamic-Bias Technique

Antonio Raffo, *Member, IEEE*, Gustavo Avolio, *Member, IEEE*, Valeria Vadalà, *Member, IEEE*, Dominique M. M.-P. Schreurs, *Fellow,* IEEE, and Giorgio Vannini, *Member, IEEE*

***Abstract*—We extend the recently proposed dynamic-bias measurement technique to the identification of non-quasi-static FET models. In particular, we propose to exploit two high-frequency tickles superimposed on the low-frequency large-signal excitation. The tickle frequencies are chosen in order to separately extract the quasi-static and non-quasi-static model parameters. As case study, we extracted and validated the model of an 800x0.35-μm² GaAs pHEMT.**

***Index Terms*— Dynamic bias, FETs, nonlinear measurements, nonlinear models, non-quasi-static models, semiconductor device measurements.**

I. Introduction

DESPITE the large number of model formulations proposed in the last decades (e.g., [1] – [3]), there are few procedures for extracting microwave transistor models. As a matter of fact, an extraction procedure is typically based on one or more measurement techniques (e.g., [3] – [5]), which allow one to observe the device behavior under different operating conditions, jointly with an extraction algorithm, which relies on analytical procedures or numerical optimization to minimize the discrepancies between model predictions and measurements. Clearly, the measurements used in the identification phase represent a set of *privileged* conditions for which the model will show its best accuracy. Among these measurements, large-signal-network-analyzer (LSNA) setups represent a very suitable solution, since LSNA enables microwave device characterization under realistic operation. It is worth noticing that although today's LSNAs enable large-signal measurements up to 67 GHz, it is not always possible to put the device under realistic operation. As an example, characterization under class-F operation requires at least three harmonic frequencies being measured and tuned and the third harmonic must not exceed the instrument bandwidth. In other words, for synthesizing class-F operation additional, expensive hardware, such as microwave multi-harmonic tuners, is required and the fundamental frequency cannot exceed 22 GHz. In order to overcome these limitations, the dynamic-bias technique was introduced in [6] and applied to class-F operation in [7]. This measurement and characterization technique consists of the possibility to capture simultaneously current and charge nonlinearities. This implies a reduction of the measurement time and of the measurement set size needed in the extraction phase compared to other techniques based on large-signal measurements (e.g., [8]). In this work we extend the dynamic-bias technique to frequencies where non-quasi-static (NQS) effects cannot be neglected. In particular, the proposed procedure preserves the great advantage of identifying the different parts of the model by using separate spectral contents.

II. Double-Tickle Dynamic-Bias Technique

The dynamic-bias technique [6] exploits the possibility of setting the traps-occupation and thermal states of the transistor by a low-frequency (LF) multi-harmonic load-pull system [5]. At LF the transistor operation, from mixing [6] to high-efficiency power amplification [7], can be simply forced avoiding the use of expensive microwave instrumentation and overcoming LSNA bandwidth limitations. Then, a high-frequency (HF) tickle is superimposed on the LF large-signal excitation for modelling the strictly-nonlinear dynamic effects (i.e., nonlinear capacitances). As shown in Fig.1, in this paper we use an additional HF tickle for modelling NQS effects. In particular, the frequency of the first tickle (f_{RF1}) is chosen in the range where the device shows a quasi-static (QS) behavior, whereas the second frequency (f_{RF2}) is set where the device manifests a clear non-quasi-static behavior.

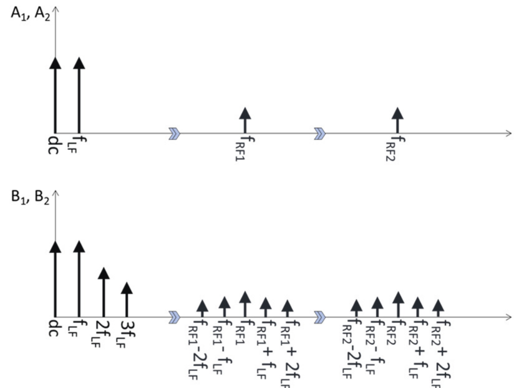

Fig.1. Illustrative frequency spectra of the incident (A1 and A2) and scattered (B1 and B2) waves under double-tickle dynamic-bias condition.

Manuscript received June 18, 2015. This work was supported by Italian MIUR and FWO – Vlaanderen (Belgium). A. Raffo, V. Vadalà, and G. Vannini are with the Department of Engineering, University of Ferrara, 44122 Ferrara, Italy (e-mail: antonio.raffo@unife.it). G. Avolio and D. M. M.-P Schreurs are with the ESAT-Divison TELEMIC, KU Leuven, B-3001 Leuven, Belgium.

It is worth noticing that, by definition [6] and due to the small-signal HF regime, the spectral content around the tickle harmonic frequencies can be neglected as well as every intermodulation product arising from the interactions between the two tickles.

The tickle frequencies can be identified in different ways. For simplicity, we suggest to look at the frequency behavior of the measured Y-parameters at the transistor intrinsic plane under class-A bias condition. As an example, Fig. 2 shows the imaginary part of the Y_{21} parameter of an 800x0.35-μm^2 GaAs pHEMT: it is clear that up to 5 GHz the device exhibits a quasi-static behavior, whereas at higher frequencies NQS effects become increasingly relevant. Since, at the beginning, the parasitic elements have to be identified, the intrinsic device is not accessible. Nevertheless, the tickle frequencies can be selected using the initial values of the model parameters, which are identified starting from a small set of dc and S-parameter measurements [6]. At the end of the extraction procedure, when the final values of the parasitic elements are available, the choice can be definitely validated or possibly adjusted.

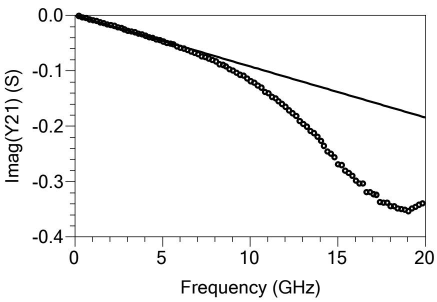

Fig.2. Measured (symbols) imaginary part of the Y_{21} parameter at the intrinsic device under class-A bias condition (i.e., V_{g0} = -0.6 V , V_{d0} = 6 V). The continuous line represents the behavior of an ideal QS device.

As transistor description, we used the Angelov model [1], whose equivalent-circuit description is reported in Fig. 3. Once the initial values of the model parameters have been estimated from DC and S-parameter measurements, the model extraction procedure is essentially based on three successive optimization steps that involve respectively:

1. The current-generator model, the conductive gate current (i.e., Schottky junction characteristic), the drain and source parasitic resistances (i.e., R_d and R_s).
2. The nonlinear capacitance model and the remaining linear parasitic elements (i.e., C_g, C_d, L_g, L_d, L_s, and R_g).
3. The model parameters that account for non-quasi-static effects.

Within the first step we minimized the discrepancies between model predictions and the gathered LF spectral components (see Fig. 1). Analogously, for the second step we optimized against the measured harmonic content around f_{RF1} and, finally, for the third step we optimized against the measured harmonic content around f_{RF2}. Within the third step we optimized only the parameters of the NQS model (τ, R_i, and R_{gd} [1]) while we kept fixed the parameters of the current generator and the nonlinear capacitances. Actually the parameter τ introduces the transcapacitance in the small-signal behavior of the device. Nevertheless, such parameter accounts for the finite memory time of the device [9], whose effect is noticeable and, as a consequence, accurately identifiable only in the NQS region.

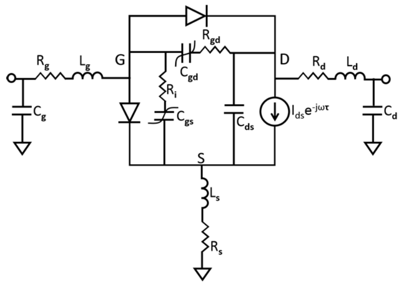

Fig.3. Nonlinear equivalent-circuit description adopted.

In conclusion, differently from [6]-[7], the proposed approach requires one additional RF tickle in the measurement phase (Fig. 1) and one additional optimization step in the extraction phase.

III. Experimental Results

With the aim of demonstrating the validity of the proposed extraction procedure, we extracted the Angelov model [1] of an 800x0.35-μm^2 GaAs pHEMT from dynamic-bias measurements under the following conditions: V_{g0} = -0.6 V, V_{d0} = 6 V, f_{LF} = 1 MHz, f_{RF1} = 4 GHz, and f_{RF2} = 15 GHz. We applied, for convenience, the HF tickles at the input port while the output port was terminated with a resistive load. The tickle power was -25 dBm. However one could also apply the HF tickles at the output port. The model parameters [10], obtained after the three-step extraction procedure described in the previous Section, are reported in Table I. In order to validate our extraction procedure, we compare the model predictions with one-tone continuous wave measurements at 15 GHz carried out for different load impedances. In Fig. 4 we report the measured load impedances at 15 GHz with the load impedances obtained by simulating the QS and NQS models. Harmonic Balance simulations were performed by forcing the measured incident waves at the device ports.

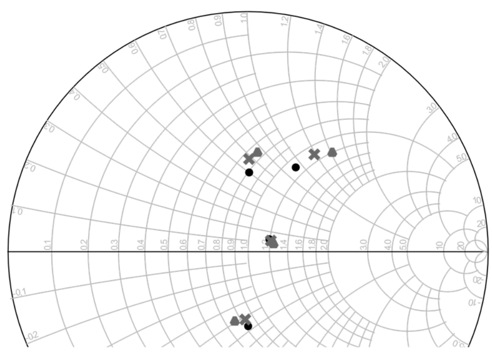

Fig.4. Measured (dots) and simulated load impedances at 15 GHz, V_{g0} = - 0.6 V , and V_{d0} = 6 V: QS model (triangles) and NQS model (crosses).

In Fig. 5 we show the measured and simulated output power corresponding to the load near the center of the Smith Chart in Fig. 4. We choose this load to demonstrate that a significant accuracy improvement in transistor performance prediction is achieved with the NQS model even when the NQS parameters have a negligible impact on the prediction of the corresponding impedance. To definitely assess the correct identification of the NQS parameters, we also carried out CW measurements at 18 GHz. The comparison between measurements and simulations reported in Fig. 6 clearly demonstrates the better prediction achievable adopting the NQS description.

IV. Conclusion

We described a new technique for extracting NQS models of microwave devices. In order to validate the proposed approach, we compared measurement data with model predictions, highlighting the accurate extraction of the parameters describing the device NQS behavior.

References

[1] I. Angelov, et al. "An empirical table-based FET model," *IEEE Trans. Microw. Theory and Techn.*, vol. 47, no. 12, pp. 2350-2357, Dec. 1999.

[2] V. I. Cojocaru and T. Brazil, "A scalable general-purpose model for microwave FET's including DC/AC dispersion effects," *IEEE Trans. Microw. Theory and Techn.*, vol. 45, pp. 2248-2255, Dec. 1997.

[3] J. Verspecht, and D. E. Root, "Poly harmonic distortion modeling". *IEEE Microw. Magazine*, vol. 7, no. 3, pp. 44-57, Jun. 2006.

[4] J.P. Teyssier, *et al.*, "40 GHz/150-ns versatile pulsed measurement system for microwave transistor isothermal characterization," *IEEE Trans. Microw. Theory and Techn.,* vol. 46, pp. 2043-2052, Dec. 1998.

[5] A. Raffo, G. Bosi, V. Vadalà, and G. Vannini, "Behavioral modeling of GaN FETs: a load-line approach," *IEEE Trans. Microw. Theory and Techn.*, vol. 62, no. 1, pp. 73–82, Jan. 2014.

[6] G. Avolio, et al., "Millimeter-Wave FET nonlinear modelling based on the dynamic-bias measurement technique," *IEEE Trans. Microw. Theory and Techn.*, vol. 62, no. 11, pp. 2526-2537, Nov. 2014.

[7] V. Vadalà, et al., "Extraction of accurate GaN HEMT model for high-efficiency power amplifier design," in *IEEE MTT-S Int. Microw. Symp. Dig.*, May 2015.

[8] G. Avolio, et al., "Identification technique of FET model based on vector nonlinear measurements," *Electronics Letters*, vol. 47, no. 24, pp. 1323-1324, Nov. 2011.

[9] A. Raffo, et al., "Electron device model parameter identification through large-signal-predictive small-signal-based error functions," *IEEE Trans. Microw. Theory and Techn.*, vol. 55, no. 10, pp. 1997–2005, Oct. 2007.

[10] Nonlinear Devices, Keysight ADS. Keysight Technol., Palo Alto, CA, 2011.

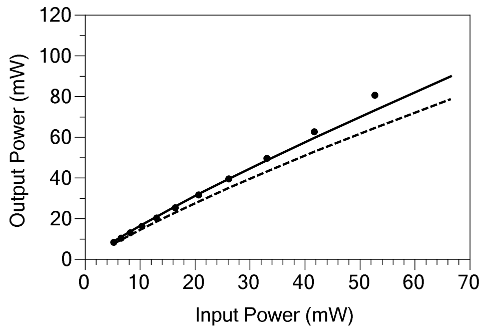

Fig.5. Measured (dots) and simulated output power at 15 GHz, V_{g0} = -0.6 V, and V_{d0} = 6 V: QS model (dashed line) and NQS model (continuous line).

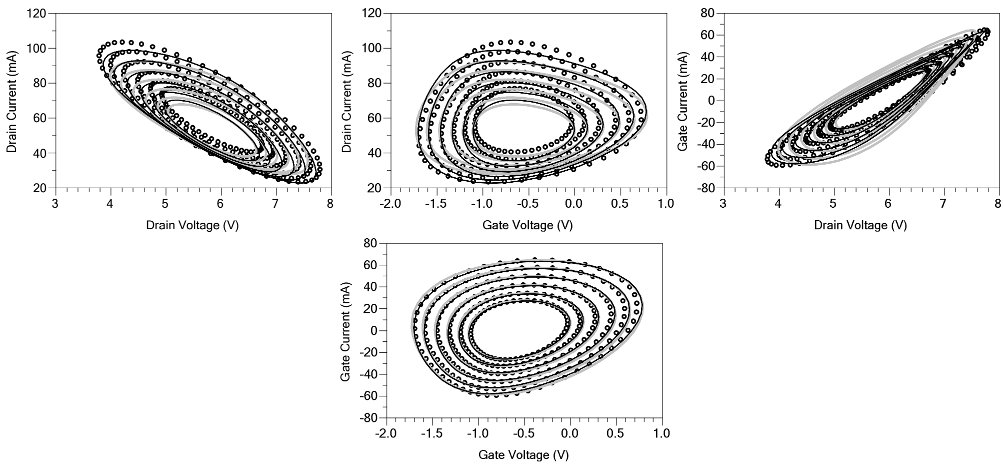

Fig.6. Measured (circles) and simulated dynamic loci for a power sweep at 18 GHz, V_{g0} = -0.6 V, V_{d0} = 6 V, and Z_L = 39.1+j31.9 Ω: QS (grey lines) and NQS (black lines) models.

TABLE I
MODEL PARAMETERS

Parasitic Elements									
	R_g (Ω)	R_d (Ω)	R_s (Ω)	L_g (pH)	L_d (pH)	L_s (pH)	C_g (fF)	C_d (fF)	
	0.61	0.42	0.05	198	205	11.4	21.78	81.27	
Current-Generator Model									
I_{pk0} (mA)	V_{pks} (V)	D_{Vpks} (V)	P_1	P_2	P_3	λ	α_R	α_S	B_1
228	0.12	0.68	1	0	0.55	0.0044	0.001	0.65	1.45
B_2	R_{th}	T_{cp1}	T_{cIpk0}						
1.13	18.5	-0.0059	-0.0006						
Nonlinear Capacitance Model: QS and NQS (bold) parameters									
C_{gspi} (fF)	C_{gs0} (fF)	C_{gdpi} (fF)	C_{gd0} (fF)	C_{ds} (fF)	P_{11}, P_{41}	P_{10}, P_{40}	P_{21}	P_{20}	P_{31}
375	172.6	185.1	170.1	197	6.5	5.6	1.05	1.32	0.1
τ (ps)	**R_{gd}** (Ω)	**R_i** (Ω)							
3.2	0.02	0.4							